

## Dependence of Peak Frequency of Microwave Absorption for Co<sub>2</sub>Z Composite on the Thickness

Guoguo Tan<sup>1, 2, a</sup>, Xisheng Gu<sup>1, 2, b</sup>, Shuwen Chen<sup>1, 2, c</sup>, Qikui Man<sup>1, 2, d,\*</sup>,  
Chuntao Chang<sup>1, 2, e</sup>, Runwei Li<sup>1, 2, f</sup>, Fashen Li<sup>1, 2, 3, g</sup>, Xinmin Wang<sup>1, 2, h</sup>

<sup>1</sup>Key Laboratory of Magnetic Materials and Devices, Ningbo Institute of Materials Technology & Engineering, Chinese Academy of Sciences, Ningbo, Zhejiang 315201, China

<sup>2</sup>Zhejiang Province Key Laboratory of Magnetic Materials and Application Technology, Ningbo Institute of Materials Technology & Engineering, Chinese Academy of Sciences, Ningbo, Zhejiang 315201, China

<sup>3</sup>Institute of Applied Magnetism, Key Laboratory of Magnetism and Magnetic Materials of the Ministry of Education, Lanzhou University, Lanzhou 730000, China

<sup>a</sup>kant01@126.com, <sup>b</sup>guxisheng@nimte.ac.cn, <sup>c</sup>chenshuwen@nimte.ac.cn, <sup>d\*</sup>manqk@nimte.ac.cn, <sup>e</sup>ctchang@nimte.ac.cn, <sup>f</sup>runweili@nimte.ac.cn, <sup>g</sup>lifs@lzu.edu.cn, <sup>h</sup>wangxm@nimte.ac.cn.

**Keywords:** Z-type hexagonal ferrite, Phase matching, Impedance, Microwave absorbing materials.

**Abstract.** A map displaying the reflection loss (RL) properties including the frequency and intensity for Co<sub>2</sub>Z barium ferrite composite was developed based on the matching model. In quarter-wavelength matching map, the number and the frequency positions of absorbing peaks presenting in RL curve for Co<sub>2</sub>Z barium ferrite composite with a certain thickness could be approximately predicted by quarter-wavelength matching model. From impedance map, the intensity of absorbing peaks in measured RL curves was analyzed. Moreover, the presence of absorbing peak in RL curve could be illustrated and understood physically and clearly using a picture of interference cancellation of two EM waves reflected by the absorber layer interface and a backed metal plate.

### Introduction

Microwave absorbing materials have been used in the telecommunication, household appliances, computers, and military equipment. The absorbing materials without a backed metal plate are generally called electromagnetic shielding material applied to electromagnetic interference shielding (EMI). Absorbers backed by a metal plate can usually improve the performance of microwave reflection and therefore greatly decrease the microwave cross section. Co<sub>2</sub>Z barium ferrite with easy-plane magnetic anisotropy are widely utilized in high-frequency absorbing materials and shielding materials [1-3].

G. H. Jonker, H. P. Wijn and P. B. Brawn fabricated Co<sub>2</sub>Z barium ferrite in Philips laboratory in 1956, and found that it possessed higher natural resonance frequency, i.e. cut-off frequency, than spinel ferrite did and the static magnetic moments aligned in an easy magnetization plane (i.e. easy plane) perpendicular to c-axis [4]. Because  $H_\phi$  in c-plane is generally considerably small, the procession of the magnetic moments easily happens when a disturbed magnetic field is applied and consequently its permeability is large [5-7]. Co<sub>2</sub>Z barium ferrite absorber is usually formed by mixing ground Co<sub>2</sub>Z particles with the adhesive. This composite with weather ability and excellent mechanical properties applies to various complicated surfaces. Therefore, Co<sub>2</sub>Z barium ferrite absorber has long been a hot topic in research and applications [8, 9]. Most of the studies focused on the dependence of RL peak frequency on absorber thickness [10-12], and few studies paid attention to the intensity variation of RL peaks.

Herein, Co<sub>2</sub>Z barium ferrite was fabricated using ceramic process and then ground to powders by ball milling. Microwave absorbing properties of Co<sub>2</sub>Z/paraffin composite in different thicknesses were measured and the number and the positions of peaks presenting in measured RL curve for Co<sub>2</sub>Z barium ferrite/paraffin composite with a certain thickness were explained by the

quarter-wavelength matching model. A complete understanding of the intensity of the peaks in measured RL curves was also presented by this model.

## Experimental Details

**Preparation and characterization of Co<sub>2</sub>Z.** Co<sub>2</sub>Z barium ferrite was prepared by solid-state reaction route and then milled for 4 hours by a vibrating ball mill with an 80 mL stainless steel milling jar and milling balls of 10 mm. The ball-to-powder weight ratio was 10:1. Ethanol alcohol (99.99% purity) was used as the milling medium. Finally, Co<sub>2</sub>Z powder/paraffin composite was prepared by mixing the powder and paraffin with 30% volume concentration of the powder and pressed into a toroidal shape with an outer diameter of 7.00 mm, an inner diameter of 3.04 mm and a thickness of about 3.00 mm. The crystal structures of two nitride powders were examined by an X-ray diffractometer (XRD, Philips X'Pert PRO) with Cu K<sub>α</sub> radiation. The morphology of the powder were characterized using a scanning electron microscope (SEM, Hitachi S-4800). Complex permeability and permittivity of as-prepared composite were measured by a vector network analyzer (VNA, Agilent E8363B) in the 0.1-18.0 GHz range.

**Microwave absorbing properties of Co<sub>2</sub>Z/paraffin composite.** The S parameters including reflection coefficient S<sub>11</sub> and transmission coefficient S<sub>21</sub> of Co<sub>2</sub>Z/paraffin composite was measured by the VNA in the 0.1-18.0 GHz range and then the complex permeability and complex permittivity of the composite were calculated by Nicolson's transmission/reflection model [13]. The reflection loss, i.e. S<sub>11</sub> parameter, of the composite backed by a metal plate was directly measured by the VNA.

## Results and Discussion

**The crystal structure and morphology of Co<sub>2</sub>Z powder.** Fig. 1(a) shows the XRD pattern of as-prepared Co<sub>2</sub>Z powder and the diffraction peaks of single Z-type Co<sub>2</sub>Z present in the pattern [9, 12]. These results indicates that high-purity and Co<sub>2</sub>Z is obtained. Fig. 1(b) shows the morphology of Co<sub>2</sub>Z powder which is mainly composed of hexagonal flakes with a thickness of approximately 100-200 nm and a length of about 2 μm.

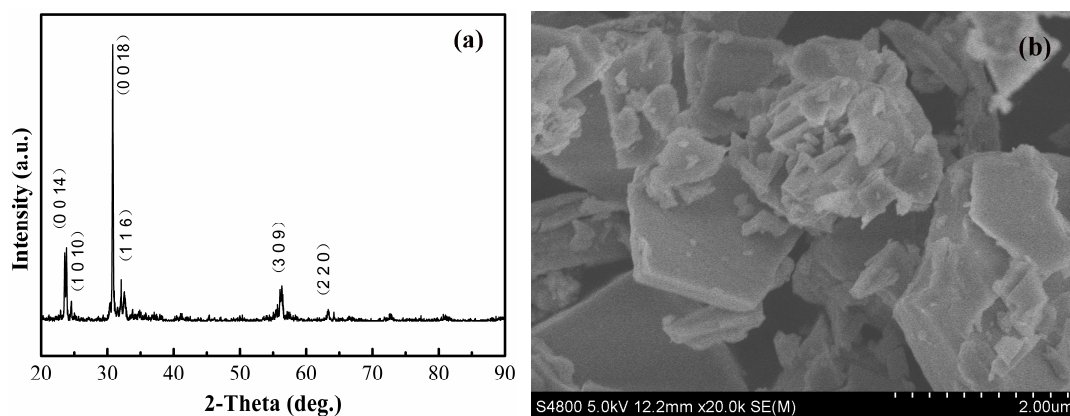


Fig. 1. (a) XRD pattern and (b) SEM picture of Co<sub>2</sub>Z powder.

**Microwave electromagnetic properties of Co<sub>2</sub>Z/paraffin composite.** The permittivity and permeability in the 0.1-18.0 GHz range of Co<sub>2</sub>Z/paraffin composite (30 vol.%) were determined as shown in Fig. 2 (a) and (b), respectively. It is found that the real part and the imaginary part of permittivity of the composite is about 4.5 and 0.2, respectively. The relaxation-type permeability was observed in Fig. 2(b) and the imaginary part of permeability reached the maximum at about 10 GHz.

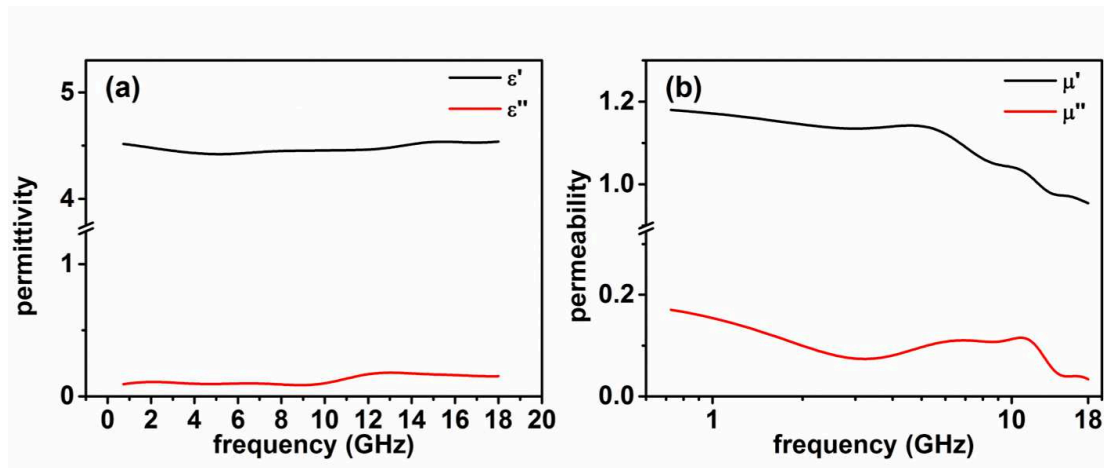


Fig. 2. (a) Complex permittivity and (b) complex permeability of  $\text{Co}_2\text{Z}$ /paraffin composite of 30% volume concentration.

RL curves (i.e. the frequency dependence of  $S_{11}$  parameter) of the composites with thicknesses of 4.95 mm, 8.69 mm and 11.27 mm backed by a metal plate were directly measured by the VNA, as shown in Fig. 3 (a), (b) and (c), respectively. From the RL curves in Fig. 3, some results can be obtained as follows: (1) When the volume concentration of the composite is given, the first peak of RL curve will shift to lower frequencies with increase of the thickness of the composite and the second and the third will present when the thickness exceeds a certain value; (2) When the thickness reaches 11.27 mm, three peaks present in the RL curve and the RL values of the second and the third peaks are smaller than the first peak, which means their absorbing-peak intensities are stronger, as shown in Fig. 3(c). Absorbing peak in RL curve was indexed using the  $i$ th-peak or  $i$ -peak from low frequency to high frequency.

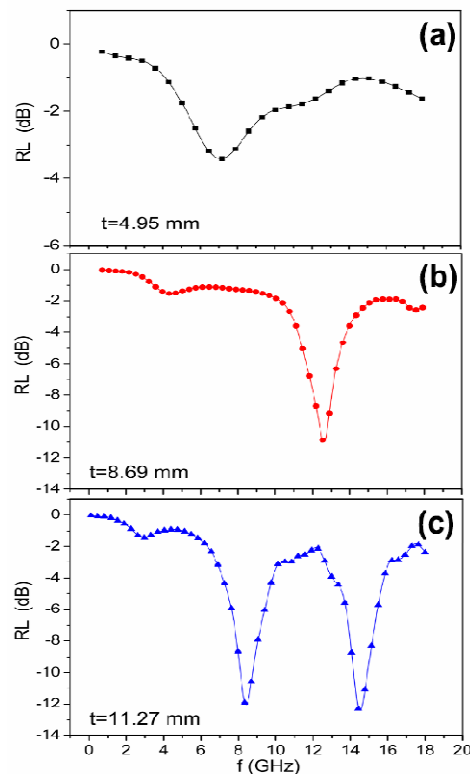


Fig. 3. Measured RL curves of  $\text{Co}_2\text{Z}$ /paraffin composite of 30% volume concentration with three thicknesses of 4.95 mm (a), 8.69 mm (b) and 11.27 mm (c).

The permeability and the permittivity of the composite with the same volume concentration are the intrinsic parameters of the composite and have no relation with the thickness. Dielectric loss and magnetic loss only depends on the imaginary parts of permittivity and permeability of the

composite, respectively. As shown in Fig. 2(b), the permittivity is basically constant and the imaginary part of permeability reaches the maximum at about 10 GHz, so the only one absorbing peak should present at 10 GHz if only two losses happen in the composite at any thickness. Therefore, the above conclusions about peaks presenting in the measured RL curves at different thicknesses cannot be explained only considering dielectric loss and magnetic loss.

**Microwave absorbing mechanism of Co<sub>2</sub>Z/paraffin composite.** From the discussion about the measured RL curves in Fig. 3, microwave absorption of Co<sub>2</sub>Z/paraffin composites backed by a metal plate cannot only be attributed to dielectric loss and magnetic loss, the more contribution results from the interference cancellation of two reflected electromagnetic (EM) waves [14, 15]. The process of the interference cancellation is described illustrated in Fig. 4 as follows: when an EM wave  $E_I$  is normally incident into the absorber backed by a metal plate, it is partly reflected by absorbing layer interface (AL interface) and then transmitted EM wave  $E_T$  is partly reflected by metal plate interface (MP interface) except for the part attenuated by the absorber, forming two EM waves of  $E_{RAL}$  and  $E_{RMP}$ , respectively. The total reflected EM wave  $E_{Rtot}$  is equal to  $E_{RAL} + E_{RMP}$ . When two reflected EM waves are out of phase by  $180^\circ$ , they cancel each other and the peak will present in the RL curve, which can be realized when the thickness of the absorber satisfies the quarter-wavelength condition shown as [16-18]:

$$t_m = \frac{nc}{4f_m \sqrt{|\epsilon_r \mu_r|}} \quad (n=1, 3, 5\dots), \quad (1)$$

where  $c$  is the velocity of light in vacuum,  $t_m$  and  $f_m$  are the matching thickness and peak frequency in RL curve, respectively, and  $\epsilon_r$  and  $\mu_r$  are the complex permittivity and permeability at  $f_m$ , respectively. The Eq. (1) is called phase matching condition of the absorber and the absorbing peak calculated by setting  $i$  to  $n$  is called an  $i$ th-level peak or  $il$ -peak.

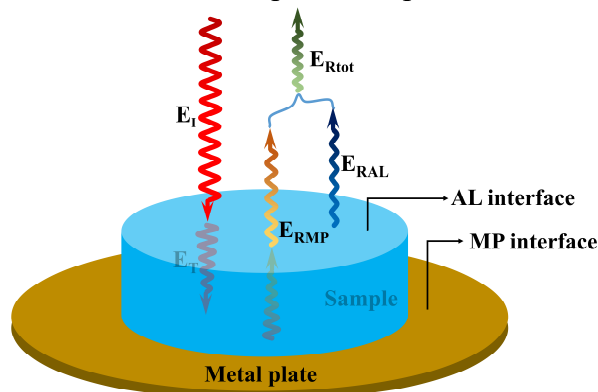


Fig. 4. Schematic diagram of the process of the interference cancellation of two reflected EM waves in an absorber backed by a metal plate.

In Fig. 5(a), three curves ( $n = 1, 3$  and  $5$ ) of matching thickness were calculated by the quarter-wavelength condition and the peak frequencies of the composite at three thicknesses of 4.95 mm, 8.69 mm and 11.27 mm were marked. The measured RL curves of the composite at three thicknesses are shown in Fig. 5(b) and the measured peak frequencies are indexed. Fig. 5(a) shows that the absorbing peak shifts to lower frequency with increase of the absorber thickness at the same matching thickness curves, which agrees with the measured result in Fig. 3. In Fig. 5(a), three thickness contours are given and the number and the frequencies of intersections of each contour and three matching thickness curves represent the number and the positions of absorbing peaks in the RL curve at the corresponding thickness, respectively. The numbers of intersections at three thicknesses of 4.95 mm, 8.69 mm and 11.27 mm are 1, 2 and 3, respectively, which agrees with the experimental result in Fig 5(b). The frequencies of intersections at each given thickness approach the measured peak frequencies at the corresponding thickness and the  $il$ -peak corresponds to the  $i$ -peak at the same thickness in Fig. 5(b). The deviation of the calculated peak frequency and the experimental one was possibly attributed to measurement errors of permeability and permittivity and the air existing between absorber and the metal plate. These results indicate that the number and

the positions of peaks presenting in measured RL curve for the composite with a certain thickness can be approximately predicted by the quarter-wavelength matching model.

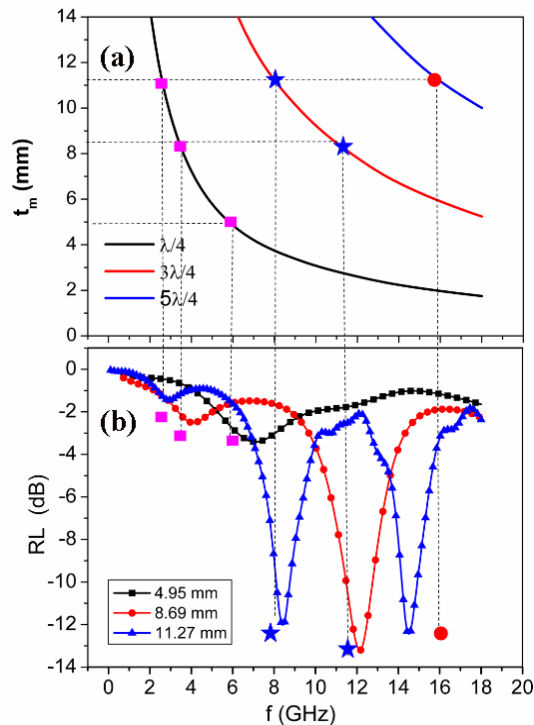


Fig. 5. (a)  $\lambda/4$ -,  $3\lambda/4$ -, and  $5\lambda/4$ -matching thickness curves calculated by the quarter-wavelength matching model and (b) peaks of measured RL curves of  $\text{Co}_2\text{Z}$ /paraffin composite of 30% volume concentration with different thicknesses.

According to the quarter-wavelength matching model, the input impedance and RL value of the absorbing peak can be calculated by transmission line theory in the case of a metal-backed single absorbing layer expressed as [19, 20]:

$$Z = Z_{in}/Z_0 = \sqrt{\frac{\mu_r}{\epsilon_r}} \tanh\left(j \frac{2\pi t}{\lambda} \sqrt{\mu_r \epsilon_r}\right), \quad (2)$$

$$RL (dB) = 20 \log \left| \frac{Z-1}{Z+1} \right|, \quad (3)$$

where  $Z_{in}$  is the input impedance of the microwave absorber,  $Z_0$  is the impedance of free space,  $Z$  is the relative impedance,  $t$  is the thickness of the absorber,  $\lambda$  is the wavelength of EM wave in free space,  $\mu_r$  is the relative complex permeability and  $\epsilon_r$  is the relative complex permittivity of the absorber. According to Eq. (3), when  $Z$  is closer to 1, the corresponding RL will become smaller and the peak intensity will get stronger. Using Eq. (1) and Eq. (2), the peak frequency dependence of matching thickness and  $|Z|$  ( $n=1, 2$ , and  $3$ ) are shown in Fig. 6. The  $|Z|$  values of  $1l$ -peaks are much larger than 1 at three thicknesses so the corresponding  $1l$ -peak intensities are weaker. The  $1l$ -peak intensity at 4.95 mm is strongest because of its  $|Z|$  values closest to 1. Similarly, because the  $|Z|$  values of  $3l$ -peaks and  $5l$ -peaks are all close to 1 at three thicknesses, intensities of corresponding  $3l$ -peak and  $5l$ -peaks are all strong and stronger than all  $1l$ -peak intensities. Therefore, the result calculated by quarter-wavelength matching model and transmission line theory coincides with the experimental measurement. Through this model,  $|Z| = 1$  can be deduced at thickness of about 14 mm and 1 GHz and 12 GHz where absorption of EM wave almost reaches 100%.

The picture of interference cancellation of two reflected EM waves as shown in Fig. 4 can be also used to illustrate and understand the results in Fig. 6 physically and more clearly. Because of low permittivity and weak conductivity of the  $\text{Co}_2\text{Z}$ /paraffin composite, the incident EM wave can penetrate easily the AL interface and amplitude of the EM reflected by AL interface is small. The attenuation constant  $\alpha$  of EM wave in an absorber is given as follows [21]:

$$\alpha = \frac{\sqrt{2}f}{c} \sqrt{\mu''\varepsilon'' - \mu'\varepsilon' + \sqrt{(\mu'^2 + \mu''^2)(\varepsilon'^2 + \varepsilon''^2)}}, \quad (4)$$

where  $c$  is the speed of light in free space,  $f$  is the frequency of the incident EM wave,  $\varepsilon'$  and  $\varepsilon''$  are real part and imaginary part of permittivity and  $\mu'$  and  $\mu''$  are real part and imaginary part of permeability. According to Eq. (4), the attenuation of EM wave in the absorber mainly depends on the frequency of EM wave and the thickness of the absorber, regardless of constant permeability and permittivity with small change in GHz. When thickness of the absorber is small equal to 4.95 mm, amplitude of  $\mathbf{E}_T$  wave is larger than  $\mathbf{E}_{RAL}$  wave and then amplitude of  $\mathbf{E}_{RMP}$  wave is also probably larger than  $\mathbf{E}_{RAL}$  wave in low frequency. Only one  $1l$ -peak presents and its intensity usually is weak as shown in Fig. 3 because  $\mathbf{E}_{RAL}$  wave cancels a little amount of  $\mathbf{E}_{RMP}$  wave. With increase of the thickness,  $1l$ -peak moves to lower frequency owing to the quarter-wavelength condition, the attenuation of  $\mathbf{E}_T$  wave and the phase difference of  $\mathbf{E}_{RAL}$  wave and  $\mathbf{E}_{RMP}$  wave increase. Consequently the second absorbing peak will present when the thickness reaches a certain value, which meets the quarter-wavelength condition. The corresponding intensity of absorbing peak probably increases owing to the decay of amplitudes of  $\mathbf{E}_{RMP}$  wave, such as the RL curve at 8.69 mm in Fig. 3. When the thickness increases further, the third absorbing peak will occur because of the similar mechanism, such as the RL curve at 11.27 mm in Figure 3. If two reflected EM wave cancel each other completely at a certain thickness, no reflected EM wave can be detected, which is known as the perfect matching.

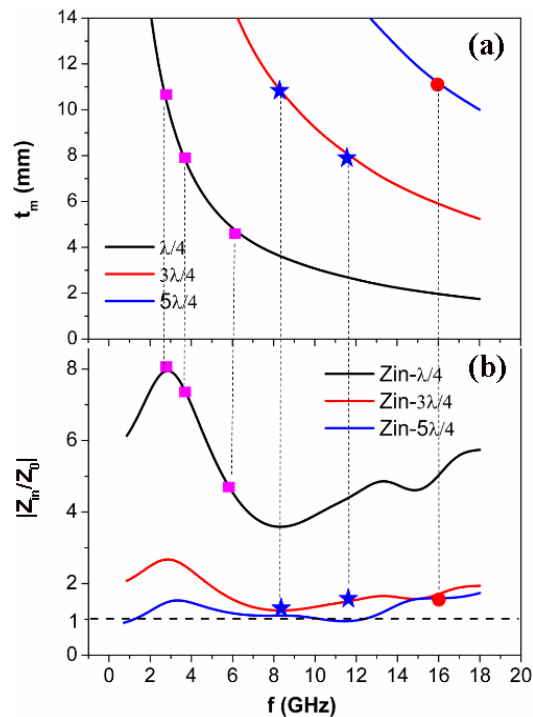


Fig. 6. (a)  $\lambda/4$ -,  $3\lambda/4$ -, and  $5\lambda/4$ -matching thickness curves and (b) the peak frequency dependence of relative input impedance  $|Z|$  calculated by quarter-wavelength matching model of  $\text{Co}_2\text{Z}/\text{paraffin}$  composite of 30% volume concentration.

## Conclusion

In this work, peak frequency dependence of reflection loss on the absorber thicknesses for  $\text{Co}_2\text{Z}/\text{paraffin}$  composite of 30% volume concentration is investigated in 0.1-18 GHz. The conclusions can be drawn as follows: (1) Interface-reflection loss mainly contributes to EM wave absorption instead of dielectric loss and magnetic loss in  $\text{Co}_2\text{Z}/\text{paraffin}$  composite; (2) The number, positions and thickness of peaks in measured RL curve (i.e.  $S_{11}$  parameter) can be explained well by the quarter-wavelength matching model; (3) The intensity of absorbing peaks in RL curve is determined by the absolute difference of amplitudes of two EM waves out of phase by  $180^\circ$

reflected by AL interface and the MP interface . When each amplitude is equivalent, two EM waves cancel each other completely and absorption of EM wave reaches 100%. In the other cases, the intensity of absorbing peak will decreases. These results are significant to the practical microwave absorption application of ferromagnetic ferrite composite.

### Acknowledgments

This work was supported by the National Natural Science Foundation of China (Grant No.51301189), Zhejiang Province Public Technology Research and Industrial Projects (Grant No.2015C31043), and Ningbo International Cooperation Projects (Grant No. 2015D10022).

### References

- [1] Z. W. Li, G. Q. Lin and L. B. Kong, *IEEE Trans. Magn.* 44, 2255 (2008).
- [2] G. Y. Chin and J. H. Wernick. *Handbook of Magnetic Materials*, Edited by Wohlfarth E P, 1980: Vol.2.
- [3] K. S. Lee, Y. C. Yun, S. W. Kim and S. S. Kim, *J. Appl. Phys.*103, 07E504 (2008).
- [4] G. H. Jonker, H. P. J. Wijn, P. B. Braun, *Proceedings of the IEE - Part B: Radio and Electronic Engineering*, 104, 249 (1957).
- [5] O. Acher, S. Dubourg, *Physical Review B*, 77 (2008).
- [6] X. De-Sheng, L. Fa-Shen, F. Xiao-Long, W. Fu-Sheng, *Chinese Physics Letters*, 25, 4120 (2008).
- [7] Y.B. Zhang, P. Wang, T.Y. Ma, Y. Wang, L. Qiao, T. Wang, *Appl. Phys. Lett.*, 108, 4 (2016).
- [8] R.C. Pullar, I.K. Bdikin, A.K. Bhattacharya, *J. Eur. Ceram. Soc.*, 32, 905 (2012).
- [9] R.C. Pullar, *Prog. Mater Sci.*, 57, 1191 (2012).
- [10] A.P. Daigle, M. Geiler, A. Geiler, E. DuPré, J. Modest, Y. Chen, C. Vittoria, V.G. Harris, *J. Magn. Magn. Mater.*, 324, 3719 (2012).
- [11] T. Wang, C. Pan, Y. Wang, G. Tan, H. Wang, R. Li, F. Li, *J. Magn. Magn. Mater.*, 354, 12 (2014).
- [12] Y. Zhang, F. Xu, G. Tan, J. Zhang, T. Wang, F. Li, *J. Alloys Compd.*, 615, 749 (2014).
- [13] A. M. Nicolsin and G. Ross, *IEEE Trans. Instrum. Meas.* 19, 377 (1970).
- [14] T. Wang, R. Han, G. G. Tan, J. Q. Wei, L. Qiao and F. S. Li, *J. Appl. Phys.*, 112, 104903 (2012)
- [15] B. C. Wang , J. Q. Wei , L. Qiao, T. Wang and F. S. Li, *J. Magn. Magn. Mater.* 324,761 (2011).
- [16] A. N. Yusoff, M. H. Abdullah, S. H. Ahmad, S. F. Jusoh, A. A. Mansor, S. A. A. Hamid, *J. Appl. Phys.*, 92, 876 (2002).
- [17] S.M. Abbas, R. Chatterjee, A.K. Dixit, A.V.R. Kumar, T.C. Goel, *J. Appl. Phys.*, 101, 074105 (2007).
- [18] S. M. Abbas, A. K. Dixit, R. Chatterjee, T. C. Goel, *J. Magn. Magn. Mater.*, 309, 20 (2007).
- [19] J. R. Liu, M. Itoh, K. Machida, *Appl. Phys. Lett.* 83, 4017 (2003).
- [20] P. Singh, V. K. Babbar, A. Razdan, R. K. Puri, T. C. Goel, *J. Appl. Phys.* 87, 4362 (2000).
- [21] F. Qin, C. Brosseau, *J. Appl. Phys.*111, 061301 (2012).